Geophysical Prospecting 32, 706–724, 1984.

STATISTICAL EVALUATION OF MT AND AMT METHODS APPLIED TO A BASALT-COVERED AREA IN SOUTHEASTERN ANATOLIA, TURKEY*

O. M. ILKISIK** and A.G. JONES***

ABSTRACT

ILKISIK, O.M. and JONES, A.G. 1984, Statistical Evaluation of MT and AMT Methods Applied to a Basalt-covered Area in Southeastern Anatolia, Turkey, Geophysical Prospecting 32, 706–724.

The efficacy of the magnetotelluric and audiomagnetotelluric (MT/AMT) methods for detailing the structure of a hypothetical geological section is investigated by using the singular value decomposition (SVD) technique. The section is representative of southeastern Turkey, which is mostly covered by basalt and is a prime area for oil exploration. One of the geological units, the Germav shale at a depth of 600 m, is a problem layer for electromagnetic surveys because of its very low resistivity (on average 3 Ωm) and highly variable thickness across the area (200–900 m). In the MT frequency range (0.0004–40 Hz) its total conductance—or, since its resistivity is known from resistivity log information, its thickness—is the best resolved model parameter. The total depth to the Germav shale and the resistivity of the Cambrian/Precambrian basement are the marginally resolved parameters. In the AMT frequency range (4–10 000 Hz) the resistivity of the surface basalt layer strongly affects the resolution of the other, less important, model parameters which are the total depth to the Germav shale and the total conductance of the Germav shale. The errors in the measurements determine the number of model parameters resolvable, and are also important for interpretation of the geological model parameters to within a desired accuracy.

It is shown that statistical evaluation of the MT and/or AMT interpretations by using an SVD factorization of the sensitivity matrix can be helpful to define the importance of some particular stage of the interpretation, and also provides a priori knowledge to plan a proposed survey. Arrangements of MT and AMT observations, together with some Schlumberger resistivity soundings, on a large grid will certainly provide three-dimensional detailed information of the deep geoelectric structure of the area.

* Received July 1983, revisions December 1983.

** Department of Geology, University of Toronto, Toronto, Ontario, M5S 1A1, Canada.

*** Department of Physics, University of Toronto, Toronto, Ontario M5S 1A7, Canada, present address: Div. of Seismology and Geomagnetism, Earth Physics Branch, Energy, Mines and Resources, 1 Observatory Crescent, Ottawa, Ont. K1A 0Y3, Canada.

Introduction

In all aspects of geophysical prospecting, survey design is of paramount importance. A statistical investigation of the likely model parameters which can be resolved by a certain technique identify those areas which will, in all probability, cause problems in the interpretation stage. Hence, prior to data collection, a study should be undertaken, for any geophysical prospecting method, to ascertain if indeed the method can resolve the primary objectives.

The authors describe such a study to determine if natural source electromagnetic techniques can resolve certain parameters of interest in a given hypothetical one-dimensional model. The model chosen is representative of the oil-bearing area of southeastern Anatolia, Turkey. This area is typical of many such around the world which cause problems for seismic techniques due to the presence of a thick basalt cover. The model is taken from the known geology of the region, and electrical resistivities are assigned to the geological strata by reference to well log information. Using a singular value decomposition of the system matrix, which relates infinitesimally small variations in the parameters to the small variations in the observations thus produced, the parameter eigenvectors and associated singular values are inspected. Due to the nature of the geoelectrical model for the region, the target zone for oil exploration proves to be invisible to geoelectrical techniques. However, it is shown that valuable information can be obtained regarding lateral variations in the basalt cover, in the Cambrian/Precambrian bedrock and in the thick Germav shale which is directly above the target zone in the geological sequence.

Theory

Consider a geoelectric model of the earth with the n parameters p_j, $(j = 1, n)$ denoting the resistivities and thicknesses of the layers. Let the observed O_i, or theoretical C_i, $(i = 1, m)$ magnetotelluric responses on the surface of the model be the apparent resistivities and/or phases at m frequencies. For infinitesimally small variations, Δp_j, in the parameters, the changes introduced in the responses, Δc_i, are given by a linearization of the functional relationship between the parameters and the observations, viz.,

$$\Delta \mathbf{c} = \mathbf{A} \cdot \Delta \mathbf{p} \tag{1}$$

where $\Delta\mathbf{c}$ is a vector of length m, $\Delta\mathbf{p}$ is a vector of length n and $\mathbf{A}$ is the $m \times n$ matrix of partial derivatives of the calculated responses with respect to the model parameters, i.e.,

$$\mathbf{A} = \left(\frac{\partial c_i}{\partial p_j}\right)_{\substack{i=1,m\\ j=1,n}}. \tag{2}$$

The matrix (2) is known as "sensitivity matrix" or "system matrix" of the problem.

Equation (1) represents a system of m linear equations in n unknowns. The solution of this problem has been discussed by Wiggins (1972) and Jackson (1972), and more recently by Edwards, Bailey and Garland (1980) and Jones (1982). If there are more data than parameters, and if there are q independent equations in (1), i.e., if the rank of $\mathbf{A}$ is q with $q < n < m$, then the system is both overconstrained and underdetermined. In order that the system matrix is not biased by any one model parameter, it must be weighted by a matrix $\mathbf{W}$, so that the parameters are equally scaled. The matrix $\mathbf{W}$ is the parameter covariance matrix and its elements are proportional to the dimensions of the parameters. Also, $\mathbf{A}$ must be scaled by a matrix $\mathbf{S}$, so that the observations have equal standard errors. Hence, the scaled system matrix $\mathbf{A}'$ is given by

$$\mathbf{A}' = \mathbf{S}^{-1/2} \cdot \mathbf{A} \cdot \mathbf{W}^{1/2} \tag{3}$$

and the parameters and observations are accordingly scaled by

$$\Delta\mathbf{p}' = \mathbf{W}^{1/2} \cdot \Delta\mathbf{p}, \tag{4}$$

$$\Delta\mathbf{c}' = \mathbf{S}^{-1/2} \cdot \Delta\mathbf{c}. \tag{5}$$

In this scaled system, the scaled parameters $\mathbf{P}'$ are dimensionless, and the scaled data $\mathbf{C}'$ all have the same variance σ_d^2. Equation (1), after transformation, becomes

$$\underset{m \times 1}{\Delta\mathbf{c}'} = \underset{m \times n}{\mathbf{A}'} \cdot \underset{n \times 1}{\Delta\mathbf{p}'}. \tag{6}$$

The scaled system matrix can be factored into three matrices $\mathbf{U}$, $\mathbf{\Lambda}$, and $\mathbf{V}$, viz.,

$$\underset{m \times n}{\mathbf{A}'} = \underset{m \times q}{\mathbf{U}} \cdot \underset{q \times q}{\mathbf{\Lambda}} \cdot \underset{q \times n}{\mathbf{V}^T}, \tag{7}$$

where matrix $\mathbf{V} \cdot \mathbf{V}^T$ is known as the resolution matrix, and is defined such that it is idempotent, i.e., $(\mathbf{V} \cdot \mathbf{V}^T)^2 = \mathbf{V} \cdot \mathbf{V}^T$, hence $\mathbf{V}^T \cdot \mathbf{V} = \mathbf{I}$ where $\mathbf{I}$ is the identity matrix and T implies transpose. Matrix $\mathbf{U} \cdot \mathbf{U}^T$ is known as the information density matrix, and is also idempotent. The matrix $\mathbf{\Lambda}$ is diagonal, and its elements are the positive square roots of the eigenvalues of $\mathbf{A}^T \cdot \mathbf{A}$ (which are also the positive square roots of the eigenvalues of $\mathbf{A} \cdot \mathbf{A}^T$), and are called the singular values of $\mathbf{A}$ (Lanczos 1961, Golub and Reinsch 1970). The decomposition given by (7) is called the singular value decomposition (SVD) of $\mathbf{A}$.

Matrix $\mathbf{U}$ contains q data eigenvectors $\mathbf{u}_i$, each of the length m, associated with the observations relating to the resolvable parameters. Diagonal matrix $\mathbf{\Lambda}$ contains q nonzero singular values λ_k, which can be ordered such that $\lambda_k > \lambda_{k+1}$. Matrix $\mathbf{V}$ contains q parameter eigenvectors $\mathbf{v}_j$ each of length n associated with the resolvable mixed model parameters. The rank q of $\mathbf{A}$ is the number of degrees of freedom, i.e., the number of resolvable mixed model parameters associated with the problem.

Obviously,

$$\Delta\mathbf{c}' = \mathbf{U} \cdot \mathbf{\Lambda} \cdot \mathbf{V}^T \cdot \Delta\mathbf{p}', \tag{8}$$

hence,

$$\mathbf{U}^T \cdot \Delta\mathbf{c}' = \mathbf{\Lambda} \cdot \mathbf{V}^T \cdot \Delta\mathbf{p}'. \tag{9}$$

Accordingly, the scaled data and parameters can be reparameterized such that we define the scaled eigendata $\mathbf{C}^*$, by

$$\mathbf{C}^* = \mathbf{U}^T \cdot \mathbf{C}', \tag{10}$$

and the scaled eigenparameters, $\mathbf{P}^*$ as

$$\mathbf{P}^* = \mathbf{V}^T \cdot \mathbf{P}'. \tag{11}$$

Hence, the infinitesimally small variations in the scaled eigenparameters, $\Delta\mathbf{p}^* = \mathbf{V}^T \cdot \Delta\mathbf{p}'$, are related directly to the resulting small changes in the scaled eigendata, $\Delta\mathbf{c}^* = \mathbf{U}^T \cdot \Delta\mathbf{c}'$, by the multiplicative singular values, viz.,

$$\Delta\mathbf{c}^* = \mathbf{\Lambda} \cdot \Delta\mathbf{p}^*. \tag{12}$$

Hence, for the kth element of $\Delta\mathbf{c}^*$ one has $\Delta c_k^* = \lambda_k \Delta p_k^*$.

This SVD factorization, with the aid of eigenvalues and eigenvectors, is an ideal way to classify the reparameterized model parameters into important, marginally important, and unimportant. The rank q is determined by the number of singular values λ_k greater than a given threshold, which may be the machine "zero". The threshold for the assignment of a certain singular value to one of the three classes (important, marginally important and unimportant) depends on the observation errors. There are two basic techniques for describing this threshold, the sharp cut-off places singular values into only two classes, namely those above ($\lambda_k > \sigma_0^2$) and those below ($\lambda_k < \sigma_0^2$) a defined problem variance σ_0^2. The tapered cut-off places a singular value into one of the three classes specified above according to the ratio $\lambda_k/(\lambda_k^2 + \sigma_0^2)$ and is akin to the stochastic inverse of Jordan (1972). The stochastic inverse was shown by Jordan (1972, see also Aki and Richards 1980, p. 706) to lie on the optimum point on the trade-off curve between resolution and variance. In this work, we use the tapered cut-off, rather than a sharp cut-off, and accordingly q is defined by

$$q = \sum_{k=1}^{n} \frac{\lambda_k^2}{\lambda_k^2 + \sigma_0^2} \tag{13}$$

(Wiggins 1972). The problem constant σ_0^2 is given by

$$\sigma_0^2 = \frac{(\Delta\mathbf{c})^T \cdot (\mathbf{I} - \mathbf{U} \cdot \mathbf{U}^T) \cdot \Delta\mathbf{c}}{m - n} \tag{14}$$

(Hamilton 1964, p. 130; Inman 1975; Lawson and Hanson 1974, p. 67) and is a measure of the misfit between the model and the observations. If $\sigma_0^2 > \sigma_d^2$, then either the variances associated with the data have been underestimated, or the model is inadequate to fit the observations. For $\sigma_0^2 < \sigma_d^2$, Wiggins (1972) suggests that the internal consistency between the observations is better than that assessed and accordingly that the variances be reduced to the point such that $\sigma_0^2 = \sigma_d^2$. We do not prescribe to this view, but consider that $\sigma_0^2 < \sigma_d^2$ indicates that the model found is one of many acceptable to the observations and accordingly if $\sigma_0^2 < \sigma_d^2$ it is reset to σ_d^2. However, for this work, as no real data are available, the matrix $\mathbf{S}$ is chosen such that σ_0^2 is always unity.

As we use the tapered rather than the sharp cut-off, the expression for the variances in the reparameterized scaled model parameters is not simply $\sigma_0^2 \mathbf{\Lambda}^{-2}$ as employed, for example, by Wiggins (1972) and Edwards et al. (1980), but is given by

$$\mathrm{Var}\,\{\mathbf{p}_k^*\} = \left(\frac{\sigma_0 \lambda_k}{\lambda_k^2 + \sigma_0^2}\right)^2. \tag{15}$$

For $\lambda_k^2 \gg \sigma_0^2$ the variance is given by σ_0^2/λ_k^2, which is equal to the variance expression used by the above-mentioned authors and the reparameterized scaled model parameter is classed as important and is well-resolved. For $\lambda_0^2 \simeq \sigma_0^2$ the variance is of the order of 1/4 and accordingly the associated $\mathbf{p}_k^*$ is classified as marginally important and is barely resolved. For $\lambda_k^2 \ll \sigma_0^2$ the associated $\mathbf{p}_k^*$ is unimportant and cannot be resolved. [In this case the inference from (15) is that the variance is small, i.e., λ_k^2/σ_0^2, which is obviously meaningless.]

Statistical evaluation of the MT or AMT interpretations by using an SVD factorization of the sensitivity matrix can be helpful to define the importance of some particular stage of the interpretation, and can also provide a priori knowledge to help the planning stage of the experiment.

In this study, in order to derive the correct scaling of the data, we define our calculated data as log $(\rho_a(f))$ and $\phi(f)$ values, with assumed standard errors of 0.25 on log (ρ_a) and $\pi/18$ radians, i.e., 10°, on phase. These are reasonable maximum error levels on the observations which can be expected with present day technology. The effect of the magnitude of the errors on the importance of parameters is discussed below.

In order to achieve correct parameter scaling, the matrix $\mathbf{W}$ is assumed to be diagonal with elements equal to the square of the model parameter, i.e., $W_{jj} = p_j^2$. Hence, $\mathbf{W}^{1/2} = \mathbf{P} \cdot \mathbf{I}$ and this has the effect of redefining the model parameters as their logarithms, i.e., $A'_{ij} = S_{ij}^{-1/2} A_{ij} W_{jj}^{1/2} = S_{ij}^{-1/2}(\partial c_i/\partial p_j)p_j \equiv S_{ij}^{-1/2}(\partial c_i/\partial \log p_j)$. Accordingly, in this study the model parameters are defined as $R_j = \log(\rho_j)$, and $H_j = \log(h_j)$. This also has appeal as the natural scales of the layer parameters are logarithmic (Weidelt 1972).

We choose two separate frequency ranges, one to simulate the magnetotelluric (MT) method of 0.0004–40 Hz (i.e., 0.025–2500 s) and the other for the audiomagnetotelluric (AMT) method of 5–10 000 Hz.

Assignment of the Geoelectric Model

We took as a hypothetical model a geological section from southeastern Turkey. A simplified geological map of the area is shown in fig. 1. There is a large zone with volcanic cover on potentially oil-bearing sediments and, accordingly, relatively little information is available from seismic methods. Consequently, our study is to test the applicability of MT/AMT techniques for such an area. Actually, this model is also representative of many geological cross-sections from east-northeast Turkey, another area which is mostly covered by volcanic materials, and of other areas around the globe.

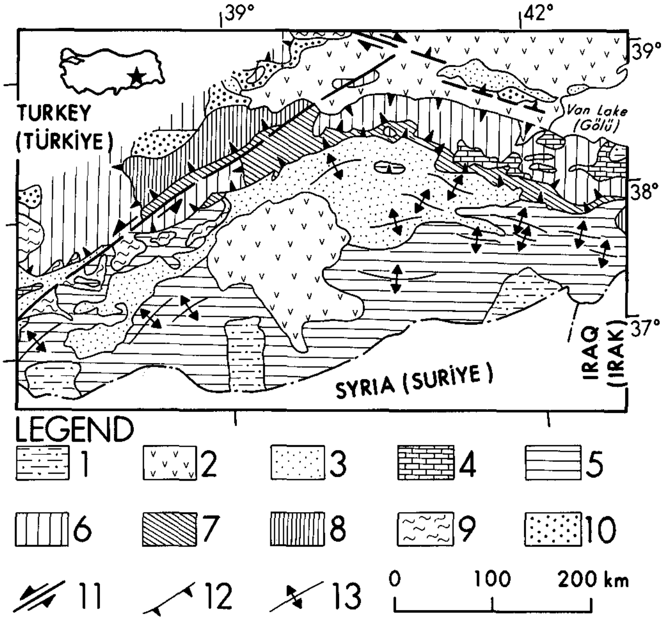

Fig. 1. Simplified geology of southeast Anatolia, Turkey, (after Sengor and Yilmaz 1981). Legend: (1) Neogene–Quaternary, (2) volcanic cover (basalt), (3) flysh (late Cretaceous–late Eocene), (4) Mesozoic autochton, (5) Mesozoic and Tertiary (Arabian platform), (6) Paleozoic autochton, (7) Ergani complex, (8) Cimmerian basement, (9) ophiolites, (10) Oligocene molasse, (11) strike-slip fault, (12) thrust fault, (13) anticline.

Using the information from Sungurlu (1974), K. Ergin (pers. comm. 1982) and M.A. Duygu, (pers. comm. 1982), the geological section was assigned various geoelectric parameters as shown in fig. 2. The superficial layer is 100–200 m thick and consists of basalt (unit 1) with a typical resistivity value of 500 Ωm. Since the resistivity of basalt can vary by an order of magnitude depending on fractures and/or fluid-fill, we assigned two different resistivity values to this zone, namely $\rho_1 = 150\,\Omega m$ and $\rho_1 = 5000\,\Omega m$. As will be shown, the resistivity of the basalt has an important effect on the interpreted models derived from the high frequency data, i.e., AMT. The second layer is Midyat limestone (unit 2) with a variable thickness, depending on the location, from 200–700 m. We assumed a thickness of 200 m for the Midyat limestone, and also 200 m for the underlying layer, the Gercus sandstones (unit 3), with assigned layer resistivities of 1000 and 600 Ωm, respectively. The fourth layer, upper and lower Germav shale (units 4a,b) is a problem layer because of its very low resistivity (*c.* 3 Ωm), and very variable thicknesses across the area (max. 900 m). For geoelectric and geomagnetic studies, it is virtually impossible to separate the upper and lower Germav shale, since both are of very similar resistivity (5 and 1 Ωm, respectively, as measured by resistivity logs). Accordingly, in this study we have merged these two layers into one layer, assigning a resistivity to the layer such that it exhibits the same total conductance (conductivity-thickness product) as

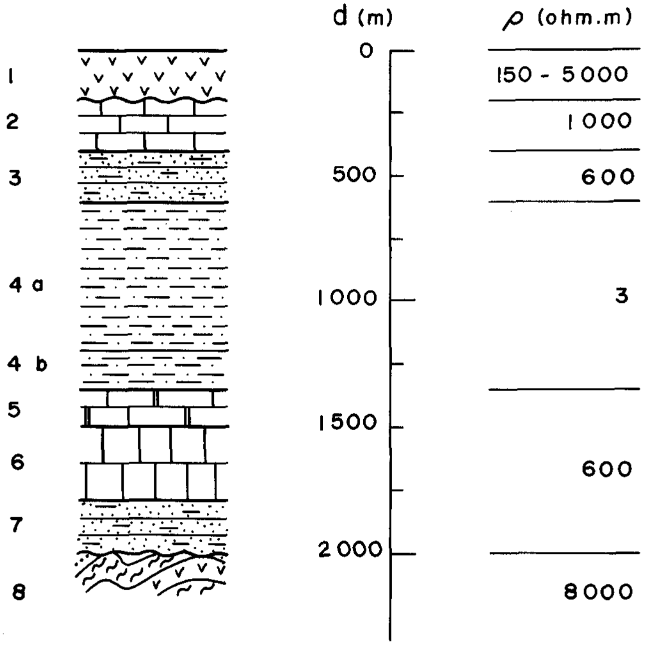

Fig. 2. A typical geological section from basalt covered area (after Sungurlu 1974; Ergin K. pers. comm., 1982; Duygu, M.A. pers. comm., 1982) and assigned geoelectric section. Legend: (1) Volcanic cover (basalt), (2) Midyat limestone, (3) Gercus sandstone, with some clay, (4a, b) Upper and lower Germav shales, (5) Garzan limestone, (6) mostly limestone Trias-Permian, (7) Ordovician sandstones, (8) Cambrian/Precambrian basement.

before. Beneath this 750 m thick Germav shale, a zone totalling 600 m of limestone, sandstone and some shale layers, occurs. This zone is the target layer for oil prospecting.

During the initial phase of the study, one fact became clear: the layers of Garzan limestone (unit 5), mostly limestone Trias-Permian (unit 6) and Ordovician sandstones (unit 7) do not have any appreciable independent effect on the magnetotelluric response of the model because of the very conductive Germav shales directly above them, and the very resistive underlying (8000 Ωm) Cambrian/Precambrian basement (unit 8). Hence, these layers (units 5–7) were also merged into one layer with an average resistivity of 600 Ωm and of the same total thickness (650 m).

The theoretical response of the above described model at the MT and AMT frequency ranges is illustrated in fig. 3. The resolution of the parameters of the model were investigated for four cases, listed in table 1, which represent AMT and MT studies over an area with a highly crystalline basalt surface layer (i.e., $\rho_1 = 5000$ Ωm, cases 1, for MT, and 3, for AMT) and, conversely, with a fractured and fissured basalt layer infilled with conducting fluid (i.e., $\rho_1 = 150$ Ωm, cases 2 and 4).

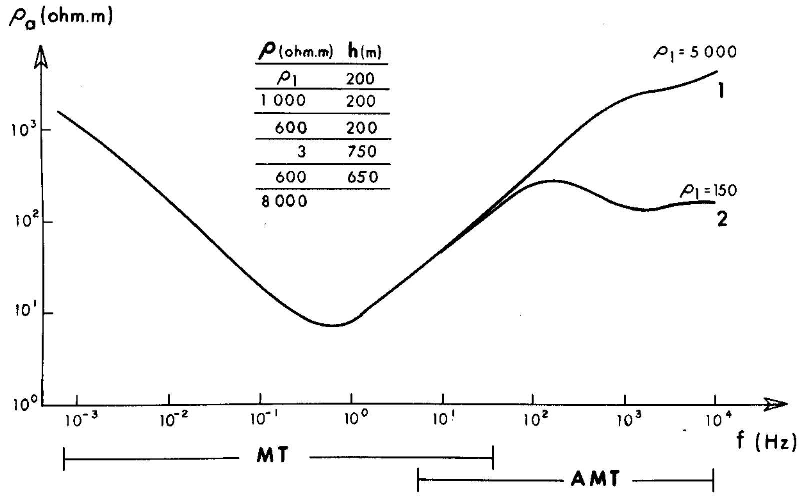

Fig. 3. The theoretical response of the adopted model (fig. 2) over the MT and AMT frequency range (0.0004–10 000 Hz) for high and low resistivity basalt cover.

Table 1. *Cases used in calculations of the theoretical response of the geologic model given in fig. 2*

Case		Frequency range (Hz)	Resistivity of basalt (Ωm)
1.	MT-1	0.0004–40	5000
2.	MT-2	0.0004–40	150
3.	AMT-1	5–10 000	5000
4.	AMT-2	5–10 000	150

Discussion of Results

The results of employing the singular value decomposition (SVD) of system matrix **A** for case 1 (MT-1) are given in table 2. The parameter eigenvectors, $\mathbf{v}_k$, and their associated singular values λ_k, $k = 1, q$ are presented graphically in fig. 4. Assuming that both the apparent resistivity and the phase are determined (with the aforementioned accuracy) one can deduce the following:

(1) The first model parameter eigenvector, i.e. that vector which indicates which mixed model parameter is best determined, consists of the terms

$$\mathbf{v}_1 = (0.00,\ -0.02,\ -0.01,\ -0.53,\ -0.03,\ -0.42,\ -0.39,\ -0.39,\ 0.49)^T$$

(note that, as mentioned previously, the matrix $\mathbf{V}^T \cdot \mathbf{V}$ is the identity matrix. Hence, the sum of the squares of the individual elements of a vector is equal to unity). Accordingly, the best resolved scaled eigenparameter p_1^*, i.e., $\mathbf{v}_1^T \cdot \mathbf{p}'$, is given by

$$p_1^* = 0.00R_1 - 0.02R_2 - 0.01R_3 - 0.53R_4 - 0.03R_5 - 0.42H_1 - 0.39H_2 - 0.39H_3 + 0.49H_4.$$

Table 2. *Singular values, parameter eigenvectors and their variances for case MT-1*

RHO matrix, i.e., $\rho_a(f)$ data alone, $q = 3.4$.

$\mathbf{v}_i$	R_1	R_2	R_3	R_4	R_5	R_6	H_1	H_2	H_3	H_4	H_5	λ_i
$\mathbf{v}_1$	0.00	0.00	0.00	**0.66**	0.00	0.03	0.33	0.33	0.32	**−0.50**	0.00	30.
$\mathbf{v}_2$	0.00	0.00	0.00	0.31	0.00	0.04	**−0.47**	**−0.47**	**−0.46**	**−0.50**	0.00	6.8
$\mathbf{v}_3$	0.00	−0.03	−0.02	0.02	0.00	**0.99**	−0.03	0.01	0.02	0.09	0.00	2.0
$\mathbf{v}_4$	0.00	−0.01	−0.01	**0.69**	0.00	−0.08	−0.11	−0.10	−0.09	**0.70**	0.00	1.3
$\mathbf{v}_5$	**−1.0**	0.00	0.00	0.00	0.00	0.00	0.00	0.00	0.00	0.00	0.00	0.15

PHA matrix, i.e., $\phi(f)$ data alone, $q = 2.3$.

$\mathbf{v}_i$	R_1	R_2	R_3	R_4	R_5	R_6	H_1	H_2	H_3	H_4	H_5	λ_i
$\mathbf{v}_1$	0.00	−0.09	−0.03	**0.75**	0.00	0.01	−0.46	−0.34	−0.31	−0.07	0.00	6.2
$\mathbf{v}_2$	0.00	−0.09	−0.03	−0.14	0.00	0.04	−0.22	−0.11	−0.08	**0.95**	0.00	1.5
$\mathbf{v}_3$	0.00	−0.23	−0.03	0.43	0.00	**−0.58**	0.10	0.40	**0.47**	0.18	0.00	1.2

TOT matrix, i.e., both $\rho_a(f)$ and $\phi(f)$ data, $q = 3.5$.

$\mathbf{v}_i$	R_1	R_2	R_3	R_4	R_5	R_6	H_1	H_2	H_3	H_4	H_5	λ_i
$\mathbf{v}_1$	0.00	−0.02	−0.01	**−0.53**	0.00	−0.03	**−0.42**	**−0.39**	**−0.39**	**0.49**	0.00	31.
$\mathbf{v}_2$	0.00	−0.02	−0.01	**0.50**	0.00	0.03	**−0.44**	**−0.41**	**−0.40**	**−0.48**	0.00	15.
$\mathbf{v}_3$	0.00	−0.11	−0.04	**0.68**	0.00	−0.05	−0.10	0.03	0.07	**0.71**	0.00	2.2
$\mathbf{v}_4$	0.00	**0.51**	0.17	0.10	0.00	**−0.57**	**0.47**	−0.19	−0.35	0.07	0.00	1.4
$\mathbf{v}_5$	**−1.0**	0.00	0.00	0.00	0.00	0.00	0.00	0.00	0.00	0.00	0.00	0.50

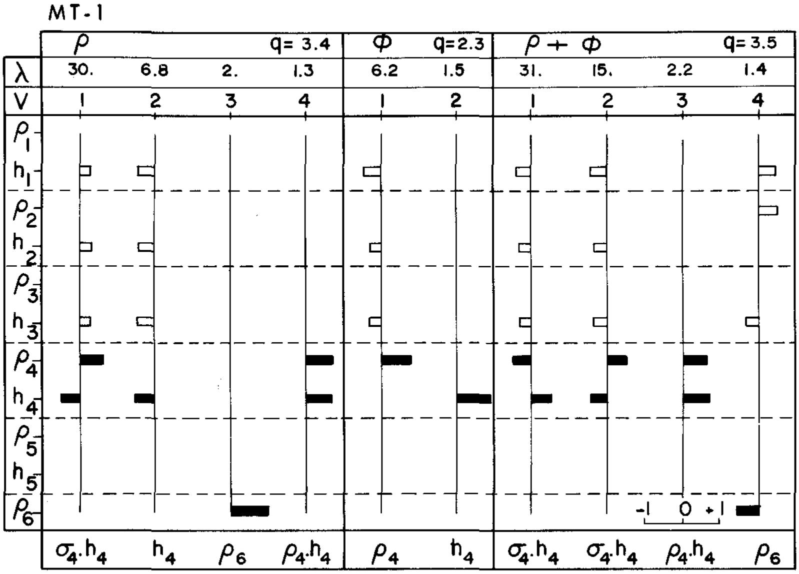

Fig. 4. The result of SVD analysis of case MT-1. The parameter eigenvectors $\mathbf{v}_i$ are given in decreasing singular value λ_k order. The resistivity and the thickness parameters given in order of layering sequence. q is the number of degrees of freedom. The eigenvectors which correponds to the most important model parameters are shown in full rectangles. Open rectangles represent marginally important parameters. The total conductance of the Germav shale is the most important parameter as is indicated by the bottom line.

(More correctly, we should associate variations in the eigenparameters with corresponding variations in the scaled model parameters, i.e., $\mathbf{v}_1^T \Delta p_1^* = 0.00\Delta R_1 - 0.02\Delta R_2 + \cdots + 0.49\Delta H_4$. However, within the range of validity of our assumption that the problem can be linearized such that (1) is valid, we are permitted to consider that $\mathbf{V}$ indicates directly the relative importance of the model parameters themselves.) Because the scaled model parameters are the logarithms of the layer resistivities and thicknesses, the sum of two model parameters which are both positive is equivalent to the multiplication of their actual layer properties. If either of the two are negative, then the resultant is the division of the two. Hence, as the contributions from R_4, H_1, H_2, H_3 and H_4 are approximately equal, this parameter eigenvector, which is the best resolved mixed model parameter for this model and in this frequency range, is equivalent to $h_4/\rho_4 h_1 h_2 h_3$. Accordingly, the conductivity-thickness product of the Germav shale S_4, given by $h_4 \sigma_4 (= h_4/\rho_4)$, is well resolved, as is a measure of the total depth to its top. However, these two are not independently determinable from this parameter eigenvector alone. The associated singular value λ_1 is 31, implying a standard error in the eigenparameter p_1^* of less than 3%.

(2) In the second parameter eigenvector, the weights of R_4, H_1, H_2, H_3, and H_4 are almost the same in magnitude as for the first parameter eigenvector, but with some differences in sign. This results in the second best resolved mixed model par-

ameter being given by $(\rho_4/h_1h_2h_3h_4)$, i.e., $1/h_1h_2h_3S_4$, which is orthogonal to the first model eigenvector $(S_4/h_1h_2h_3)$ and thus S_4 and $h_1h_2h_3$ can be independently determined. The singular value λ_2 is 15, indicating a standard error in p_2^* of less than 6%.

(3) The effect of the depth integrated resistivity of Germav shale, (i.e. $T_4 = \rho_4 h_4$) dominates in the third eigenvector by

$$\ldots, 0.68R_4, \ldots, 0.71H_4, \ldots,$$

and accordingly this eigenparameter is equivalent to T_4. Hence, the resistivity (ρ_4) and thickness (h_4) of the shale can be independently determined from the three resolvable eigenparameters. However, the singular value for p_3^* is 2.2, classifying this eigenparameter as marginally important and inferring a standard error of around 35%. These results imply that in layer 4, the good conducting Germav shale zone, the orthogonal layer parameters are not the resistivity ρ_4 and thickness h_4 but the resistivity-thickness product $T_4 = \rho_4 h_4$ and the conductivity-thickness product $S_4 = \sigma_4 h_4 = h_4/\rho_4$. Accordingly, a Dar Zarrouk parameterization of this layer, i.e., in terms of T and S, should have been used.

(4) Since the number of the degrees of freedom q (i.e., the rank of **A**) is 3.5, the fourth eigenvector gives us the last resolvable information in this analysis. This eigenparameter (with an associated singular value of 1.4) consist of the relatively important terms

$$p_4^* = 0.51R_2 + \cdots - .57R_6 + \cdots + 0.47H_1 + \cdots - .37H_3.$$

Hence, R_6, which represents the resistivity of the basement rocks, is just barely resolvable and is classed as a marginally important model parameter. Thus, only in those areas where the Germav shale thickness is small can we detect lateral variations within the basement.

(5) The model parameters corresponding to the target zone, i.e., layer 5 which is an amalgam of units 5, 6, and 7, dominate the two worst-resolved parameter eigenvectors. These eigenvectors have associated singular values of less than 0.0025, indicating that parameters ρ_5 and h_5 are totally unresolvable.

For each of the four cases under investigation, the SVD analysis results are illustrated in figs 4–7. The eigenvectors are given in the order of decreasing singular value λ_k. The most important parameters for each parameter eigenvector $\mathbf{v}_k$ are represented by full rectangles, and marginally important parameters in the same eigenvector are shown with open rectangles. The length of the rectangles indicate their contribution to the parameter eigenvector. The value of q is the number of degrees of freedom. The resolvable parameters, or parameter combinations, appear on the bottom line for the three cases when the survey has resulted in apparent resistivity data only, phase data only, and both apparent resistivity and phase data.

The results for case 1 (MT-1), as discussed above, are illustrated in fig. 4. Apparent is the strong effect of the total conductance of the Germav shale (unit 4) on the MT response. Since we know a priori the resistivity ρ_4 of this layer from resistivity log information, the lateral variation of the thickness h_4 of this layer is the best resolved model parameter.

The order of importance of the parameters resolved for our model, as discussed above, in the 0.0004–40 Hz frequency range (MT) and for the model illustrated in fig. 2, is:

1. Total conductance of the Germav shale $\sigma_4 h_4$.
2. A measure of the total depth to the Germav shale $(h_1 h_2 h_3)$ (from resistivity data).
3. Thickness of the Germav shale h_4 (from resistivity data).
4. Resistivity of the Germav shale ρ_4 (from phase data).
5. Resistivity of the Cambrian/Precambrian basement ρ_6.

Although some of the contributions to the parameter eigenvectors differ slightly for MT-2 (case 2, see fig. 5), one can say after examining the results more carefully that there is virtually no difference for the important parameters. Hence, any lateral resistivity variations of the surface basalt layer is not a very important parameter for interpreting the magnetotelluric sounding curves.

In figs 6 and 7 are similar presentations of the parameter eigenvalues for AMT-1 and AMT-2 (cases 3 and 4), respectively. In the audiofrequency range (4–10 000 Hz) the resistivity of the surface basalt layer strongly affects the resolution of the other model parameters. If this layer has a high resistivity (ρ_6 = 5000 Ωm), then $h_1 h_2 h_3$ (i.e., a measure of the total depth to Germav shale) is the most well resolved parameter (fig. 6). The total resistance of basalt layer (ρ_1) is next best resolved and the conductance of Germav shale (S_4) is the other important parameter. For a relatively conducting basalt layer at the surface (ρ_1 = 150 Ωm, fig. 7) the total

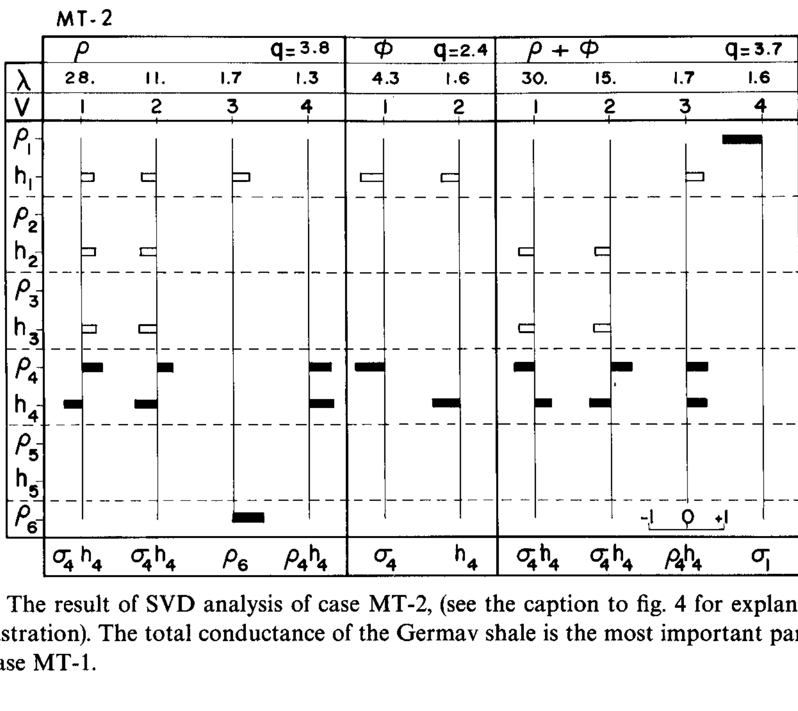

Fig. 5. The result of SVD analysis of case MT-2, (see the caption to fig. 4 for explanation of the illustration). The total conductance of the Germav shale is the most important parameter, as in case MT-1.

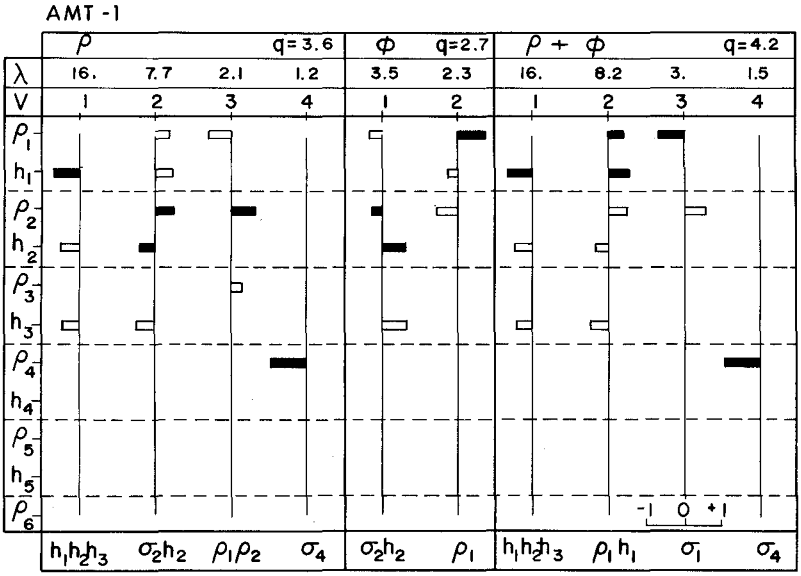

Fig. 6. The result of SVD analysis of case AMT-1. The most important parameter is the total depth to Germav shale (see fig. 4).

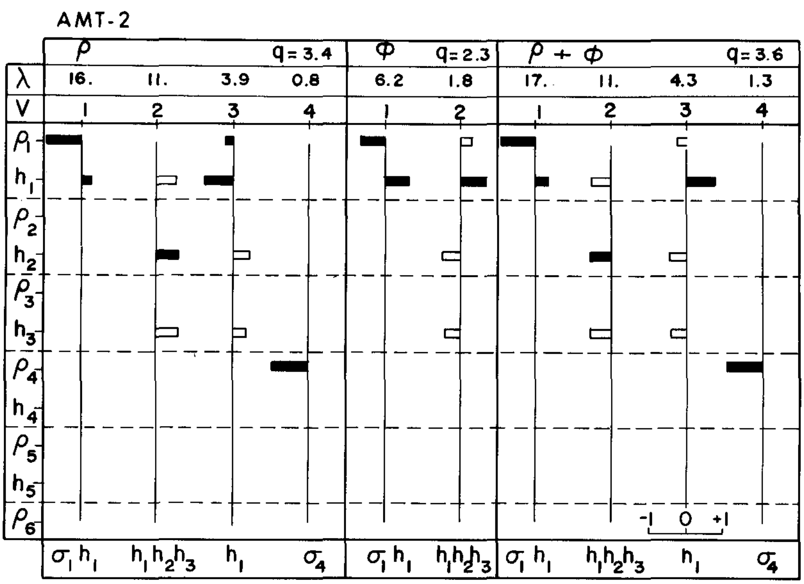

Fig. 7. The result of SVD analysis of case AMT-2. The most important parameter is the total conductance of the basalt layer (see fig. 4).

conductance of this layer ($S_1 = h_1/\rho_1 = h_1\sigma_1$) is the most important parameter for the inversion process and, hence, can be derived most precisely. Parameter $h_1 h_2 h_3$ is the next well-resolved parameter. It is also possible to resolve h_1, i.e., the thickness of the basalt layer, separately. The least well-resolved model parameter is the total conductance of Germav shale (S_4), as in the previous case.

These studies show that the variation of the depth to the Germav shale and lateral variations in the electrical resistivity of the surface layer, that are mostly due to faulting within the basalt, can be detected by an audiomagnetotelluric (AMT) survey. The resistivity of the Germav shale can also be resolved, hence lateral discontinuities within this layer (if they exist) could be located.

At some locations apparent resistivity and phase data may be available over the whole frequency range, i.e., 0.0004–10 000 Hz. In such a situation, the SVD analyses show that the total conductance of the Germav shale is again the best resolved model parameter. Remaining less important parameters are the total depth to Germav shale and the resistivity value of the basalt layer.

The effects of a variation in the important model parameters on the response curves, i.e., the partial derivatives $[\partial \log(\rho_a(f))/\partial \log(p_j))$, for each case are illustrated in figs 8–10. The parameters were chosen on the basis of the previous descrip-

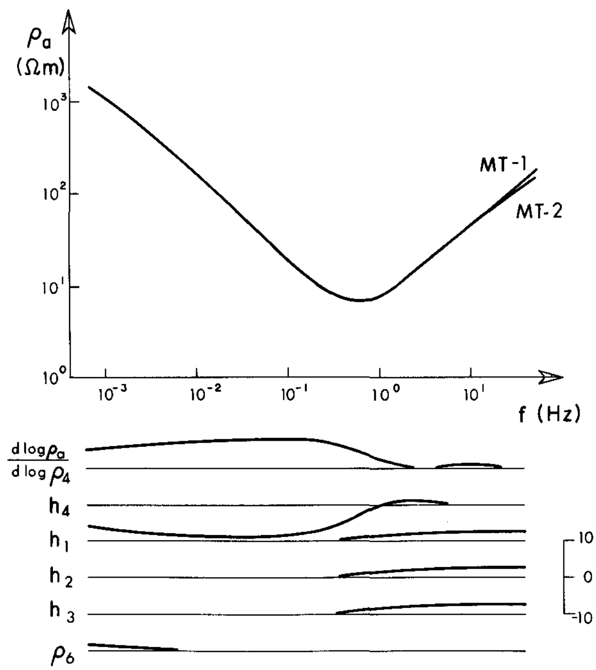

Fig. 8. The theoretical responses of cases MT-1 and MT-2 in the magnetotelluric frequency range. The plots of the effects of important model parameters show the effective frequency range for sensitivity of each model parameter on response curve. The total conductance $S_4 = h_4/\rho_4$ of the Germav shale is sensed for lower frequencies, i.e., <1 Hz. Total depth ($h_1 h_2 h_3$) to this layer is important at high frequencies.

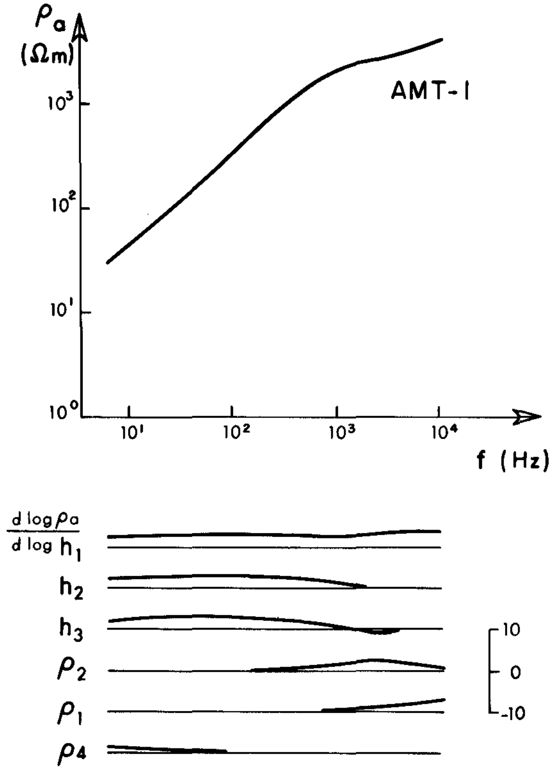

Fig. 9. The theoretical response of case AMT-1 and the effects of important model parameters. The total depth to Germav shale is the most important model parameter.

tions for each case. The figures show the effective frequency range for the sensitivity of the response curve to each model parameter. As shown in fig. 8 (cases MT-1 and MT-2), the total depth to Germav shale ($h_1 + h_2 + h_3$) affects the magnetotelluric response at frequencies greater than 1 Hz. The total conductance ($h_4 \sigma_4$) of the Germav shale is sensed at frequencies less than 1 Hz. The resistivity of the basement becomes resolvable at very low frequencies. If the thickness of Germav shale is less than 600 m (our model) in some areas, we can resolve lateral variations in Cambrian/Precambrian basement.

It is interesting to note that for AMT-1 ($\rho_1 = 5000$ Ωm) the thickness of the basalt layer affects the AMT response curve at all frequencies (fig. 9). Additionally, for the 10–1000 Hz frequency range, the effects of thicknesses h_1, h_2 and h_3 cannot be separated. Variations in ρ_1 and ρ_2 appear at high frequencies (100–10 000 Hz), and changes of ρ_4 appears at low frequencies (5–50 Hz).

If the basalt layer has a resistivity value of around 150 Ωm (AMT-2), then the effect of its resistivity is important only at very high frequencies (fig. 10). The total depth to the Germav shale ($h_1 + h_2 + h_3$) is important over the whole frequency range.

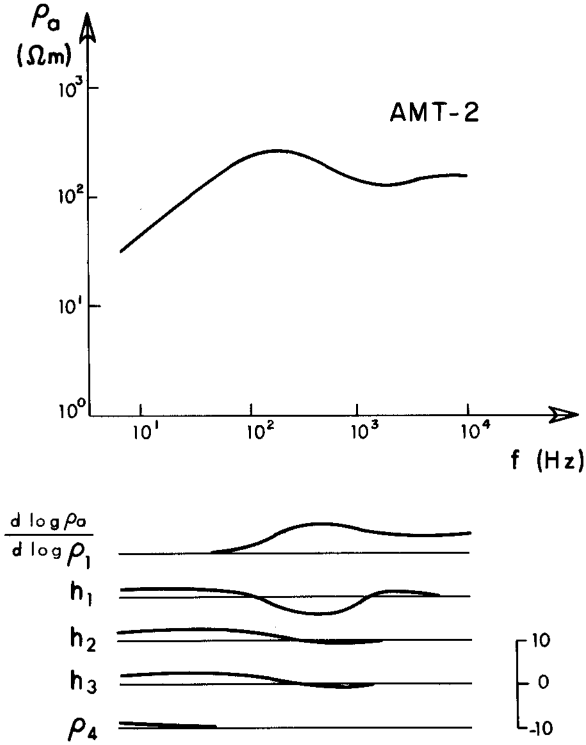

Fig. 10. The theoretical response of case AMT-2 and the effects of important model frequencies. The total conductance of the basalt layer and the depth to Germav shale are important.

Effect of Observation Errors on Interpretation

The data with the assumed standard errors of 25% for log $[\rho_a(f)]$ and 10° for $\phi(f)$ cannot provide more than four resolvable parameters of our model. This means that we cannot estimate certain parameters of our model with any reasonable accuracy (i.e., with a standard error less than 100%). The number of model parameters which could be resolved by an inversion procedure increases with decreasing standard errors of the observations. This functional relationship is slightly different for different geoelectric models or different frequency ranges. For our cases MT-1 and AMT-2, the degree of freedom coefficients v. various observation error levels are presented in table 3. A drop from 25% to 5% standard error on log ρ_a data resulted in an increase from $q = 3.5$ to $q = 4.2$, for the MT data. For AMT data, such an increase in precision results in an increase in the degree of freedom from 3.6 to 4.9, which is important as one more model parameter can be resolved, which is in this case the thickness of the Germav shale (h_4).

Depending on the grid spacing, an arrangement of various techniques (e.g., MT,

Table 3. *The degree of freedom* (q) *for different observation error levels for cases MT-1 and AMT-2*

MT-1 ($\rho_a = 5000\ \Omega$m).

Error in $\rho_a(f)$ (%)	Error in $\phi(f)$ (°)	$\rho_a(f)$ data only	$\phi(f)$ data only	both $\rho_a(f)$ and $\phi(f)$ data
25	10	3.4	2.3	3.5
15	5	3.8	2.8	4.0
10	4	3.9	3.0	4.1
5	3	4.0	3.1	4.2

AMT-2 ($\rho_a = 150\ \Omega$m).

Error in $\rho_a(f)$ (%)	Error in $\phi(f)$ (°)	$\rho_a(f)$ data only	$\phi(f)$ data only	both $\rho_a(f)$ and $\phi(f)$ data
25	10	3.4	2.3	3.6
15	5	3.8	2.9	4.1
10	4	4.1	3.1	4.4
5	3	4.8	3.3	4.9

AMT, Schlumberger or some seismic techniques) and target information, the error levels of MT/AMT measurements are important for interpretation of geoelectric model parameters to within a desired accuracy.

Conclusions

The parameter eigenvectors and their associated eigenvalues are very useful in determining the relationship between model parameters, and also their overall effect on the data generated from a model. The authors have chosen an area of known oil-bearing sediments, and have shown that a magnetotelluric survey, supplemented by many audiomagnetotelluric soundings, can give potentially useful information concerning the lateral variation of some of the geoelectric properties of the area, whereas the usual seismic methods would experience great difficulty due to the thick basalt cover.

The total conductance of the Germav shale (unit 4)—or, since we know its resistivity from resistivity log information, the thickness of the Germav shale—is the best resolved model parameter of any magnetotelluric study (frequency range 0.0004–40 Hz). The other important model parameters are the resistivity of the basement and the total depth to the Germav shale.

In the audiofrequency range (4–10000 Hz), the resistivity of the basalt layer strongly affects the importance of the other model parameters. The total depth to the Germav shale is the next well-resolved parameter. The least well-resolved parameter is the total conductance of Germav shale. Hence, this study shows that the variation of the depth to Germav shale and lateral resistivity variations (mostly faults) within the basalt layer can be detected with the audiomagnetotelluric technique. Any lateral discontinuities within the Germav shale could also be delineated. Although the actual target layer for the oil industry underlies the Germav shale and is not directly detectable, a combination of magnetotelluric and audiomagnetotelluric techniques in the area will certainly provide very valuable information on the resistivity and thickness variations of the basalt cover, and lateral variations of the depth and the thicknesses of Germav shale. In the areas where its thickness is less than 600 m, then an MT/AMT survey will also yield information on any lateral variations of target layers, and especially Cambrian/Precambrian basement rock.

Since in both frequency ranges (MT and AMT), the technique is sensitive to lateral variations in resistivity, the logistics to employ would be to make measurements on a regular grid, rather than single stations or profiles.

Finally, it is also possible to apply a similar type of statistical evaluation of the resolvable parameters of a model for controlled source electrical methods such as DC resistivity sounding (see Edwards et al. 1980). Although the eigenparameters might not be very different, such a coordination of techniques is an advantage in joint inversion of the data (Vozoff and Jupp 1975).

Acknowledgements

One of the authors (MI) wishes to thank Prof. D.W. Strangway for many useful discussions, whilst AGJ is indebted to the Natural Sciences and Engineering Research Council for funding (NSERC grants to Professors G.D. Garland (NSERCC A2115), R.N. Edwards and G.F. West (NSERCC G0501)). The computations were undertaken on the Physics VAX 780 research computer of the University of Toronto.

References

Aki, K. and Richards, P.G. 1980, Quantitative Seismology: Theory and Methods Vol. II. W.H. Freeman and Co., San Francisco.

Edwards, R.N., Bailey, R.C. and Garland, G.D. 1980, Crustal and upper mantle conductivity studies with natural and artificial sources, in The Continental Crust and its Mineral Deposits, ed. D.W. Strangway, Special Paper 20, Geological Association of Canada, 255–271.

Golub, G.H. and Reinsch, C. 1970, Singular value decomposition and least squares solutions, Numerical Mathematics 14, 403–420.

Hamilton, W.C. 1964, Statistics in Physical Sciences, Estimation, Hypothesis Testing and Least-Squares, Ronald Press Co., New York.

Inman, J.R. 1975, Resistivity inversion with ridge regression, Geophysics 40, 798–817.

Jackson, D.D. 1972, Interpretation of inaccurate, insufficient, and inconsistent data, Geophysical Journal of the Royal Astronomical Society 28, 97–109.

Jones, A.G. 1982, On the electrical crust-mantle structure in Fennoscandia: no Moho, and the asthenosphere revealed?, Geophysical Journal of the Royal Astronomical Society 68, 371–388.

JORDAN, T.H. 1972, Estimation of the radial variation of seismic velocities and density in the Earth, PhD thesis, Californian Institute of Technology, Pasadena.

LANCZOS, C. 1961, Linear Differential Operators, D. Van Nostrand Co., London, pp. 564.

LAWSON, C.L. and HANSON, R.J. 1974, Solving Least Squares Problems, Prentice-Hall Inc., New Jersey, pp. 340.

SENGOR, A.M.C. and YILMAZ, Y. 1981, Tethyan evolution of Turkey: A plate tectonic approach, Tectonophysics, 75, 181–241.

SUNGURLU, O. 1974, VI. Bolge kuzeyinin jeolojisi ve petrol imkanlari, Turkiye Ikinci Petrol Kongresi, eds H. Okay and E. Dilekoz publ. Ankara, 85–107.

WEIDELT, P. 1972, The inverse problem of geomagnetic induction, Journal of Geophysics 38, 257–289.

WIGGINS, R. 1972, The general linear inverse problem: Implications of surface waves and free oscillations for earth structure, Reviews of Geophysical Space Physics 10, 251–285.

VOZOFF, K. and JUPP, D.L.B. 1975, Joint inversion of geophysical data, Geophysical Journal of the Royal Astronomical Society 42, 977–991.